CHAPTER 8

PHARMACOPHORE MODELING, DOCKING AND VIRTUAL SCREENING OF ACETYLCHOLINESTERASE INHIBITORS

8.1 Introduction

Alzheimer's disease is a progressive and fatal neurodegenerative disorder manifested by cognitive and memory deterioration, progressive impairment of activities of daily living, a variety of neuropsychiatric symptoms and behavioural disturbances [8.1]. Acetylcholinesterase (AChE) inhibitors are the only major drugs approved for the symptomatic treatment of Alzheimer's disease [8.2]. AChE is predominantly present in the central, peripheral nervous system and in skeletal muscles. It causes the termination of impulse transmission by rapid hydrolysis of acetylcholine to yield acetic acid and choline [8.3, 8.4]. Lower level hydrolysis of the neurotransmitter acetylcholine, is a feature associated with Alzheimer's disease [8.5]. There is a steady-state increase in acetylcholine resulting from cholinesterase inhibition in the brain resulting in improvement of cognitive function and mild-to-moderate cases of Alzheimer's disease [8.6]. Therefore cholinesterase inhibitors stabilize Alzheimer's disease. Hence, AChE inhibition is deemed a useful strategy in the design and development of drug candidates for the treatment of Alzheimer's disease, as exemplified by the first approved drug, tacrine. A diverse set of compounds binds to this catalytic site and ellicit the catalytic process shown in Scheme 8.1 [8.7]. Two inhibitors, donepezil and tacrine have been successfully used clinically for AChE inhibition.

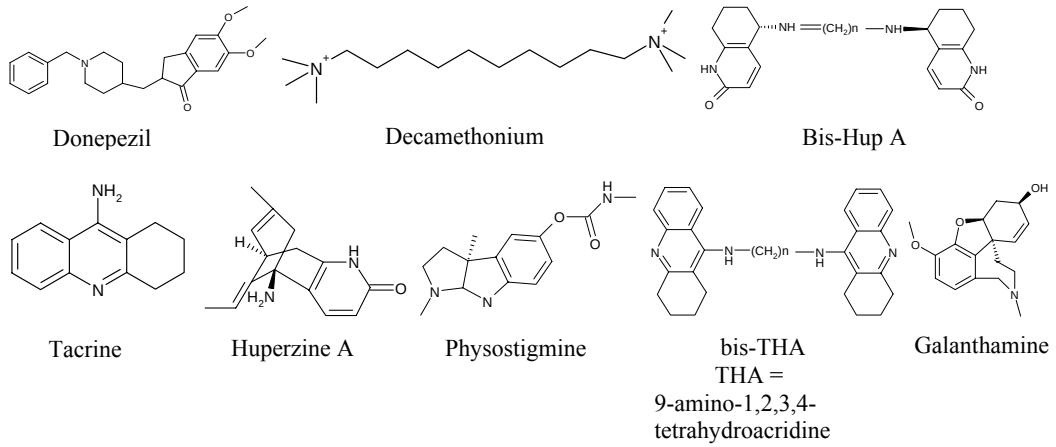

Scheme 8.1: Known AChE inhibitors.

AChE is among the best studied targets with molecular modeling. Many computational studies such as theoretical [8.8], molecular dynamics simulations (MD) [8.9], quantitative structure activity relationship (QSAR) [8.10], docking [8.11] and virtual screening (VS) [8.12] have been performed on AChE. The scope of the present work lies in the determination of a virtual screening (VS) method and its application for the system of choice. The aim of the present chapter is to develop a virtual screening (VS) model that can combine both the accuracy of docking and the speed of the pharmacophore method for the AChE inhibitor.

8.2 Materials and methods

8.2.1 *Structure building*

A data set of 153 unique AChE inhibitors was prepared with the MOE software [8.13]. These inhibitors were collected from published papers in various journals. The inhibitors include morpholinoalkylcarbamoyloxyeseroline derivatives (11 compounds) [8.14], pyripyropene (12 compounds) [8.15], E2020 analogues as acetylcholinesterase (14 compounds) [8.16], piperidinium and pyridinium agents (30 compounds) [8.17], 11H-indeno-[1,2-b]-quinolin-10-ylamine derivatives (18 compounds) [8.18], N-benzylpiperidine aminoacid derivatives (15 compounds) [8.19], Velnacrine thiaanalogues (13 compounds) [8.20], 9-amino-1,2,3,4-tetrahydroacridine-based quaternary salts of 2-[(hydroxyimino)methyl]imidazole (9 compounds) [8.21], 1-(alkoxymethyl)-2-[(hydroxyimino)methyl]-3-methylimida zolium halides (12 compounds) [8.22], tacrine analogues (19 compounds) [8.23]. The activity profile of the above mentioned compounds is shown in Figure 8.1. The chemical structures and corresponding references of these analogues are mentioned in Appendix III, Table 1.

For these inhibitors, geometry optimizations and minimizations were carried out using the MMFFx force field in MOE [8.24]. The optimized ligands were exported to Catalyst 4.7 for pharmacophore generation [8.25]. The conformations for each inhibitor were generated with the best conformation option in the Catalyst ConFirm module. A maximum of 250 conformations were generated for each molecule within an energy threshold of 20.0 kcal/mol above the global energy minimum. Pharmacophore modeling in Catalyst was carried out with the *HypoGen* module and the docking study was performed with GOLD 3.0 [8.26].

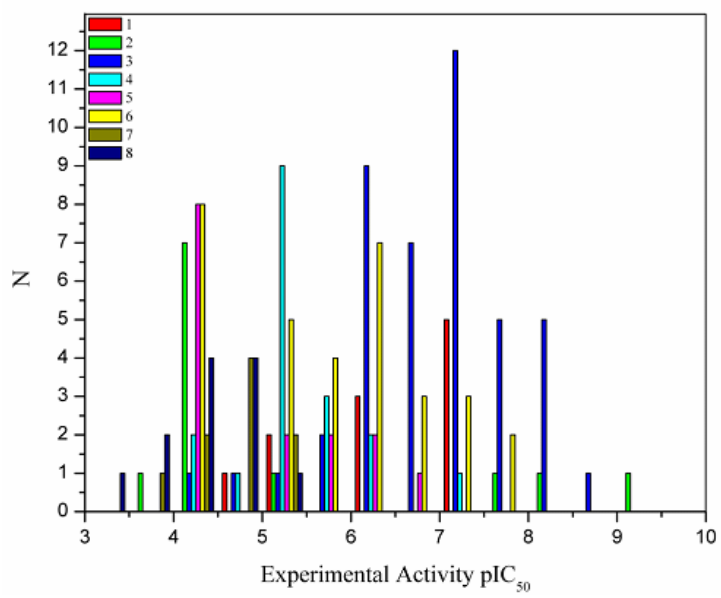

Figure 8.1: Frequency distribution of experimental activities for inhibitors, **1**: Morpholinoalkylcarbamoyloxyeseroline derivatives, **2**: pyripyropene, **3**: E2020 analogues, piperidinium and pyridinium agents, **4**: 11H-indeno-[1,2-b]-quinolin-10-ylamine derivatives, **5**: N-benzylpiperidine aminoacid derivatives, **6**: Velnacrine thiaanalogues and tacrine analogues, **7**: quaternary salts of 2-[(hydroxyimino)methyl]imidazole, **8**: 1-(alkoxymethyl)-2-[(hydroxyimino)methyl]-3-methylimida zolium halides.

8.2.2 *HypoGen*

The training set was randomly selected from the data set and is shown in Figure 8.2. The reported experimental activities were converted to pIC_{50} values. The inhibitory activities (pIC_{50}) of the selected compounds range from 8.5 to 3.4. The pharmacophore model was constructed using chemical features like hydrogen bond acceptor (HBA), hydrophobic aliphatic (HYA), ring aromatic (RA) and positive ionizable (PI). Pharmacophore generation was allowed to have a maximum of 5 features. The default uncertainty value of 3 was specified for each compound. *HypoGen* generates pharmacophore models that are a set of features in 3D space, each containing a certain tolerance and weight that fits to the features of the training set, and further correlates to the activity. This is carried out by comparing features which are common among the active compounds but not present in the inactive compounds. The best *HypoGen* model was used to predict the activity of 125 inhibitors present in the data set.

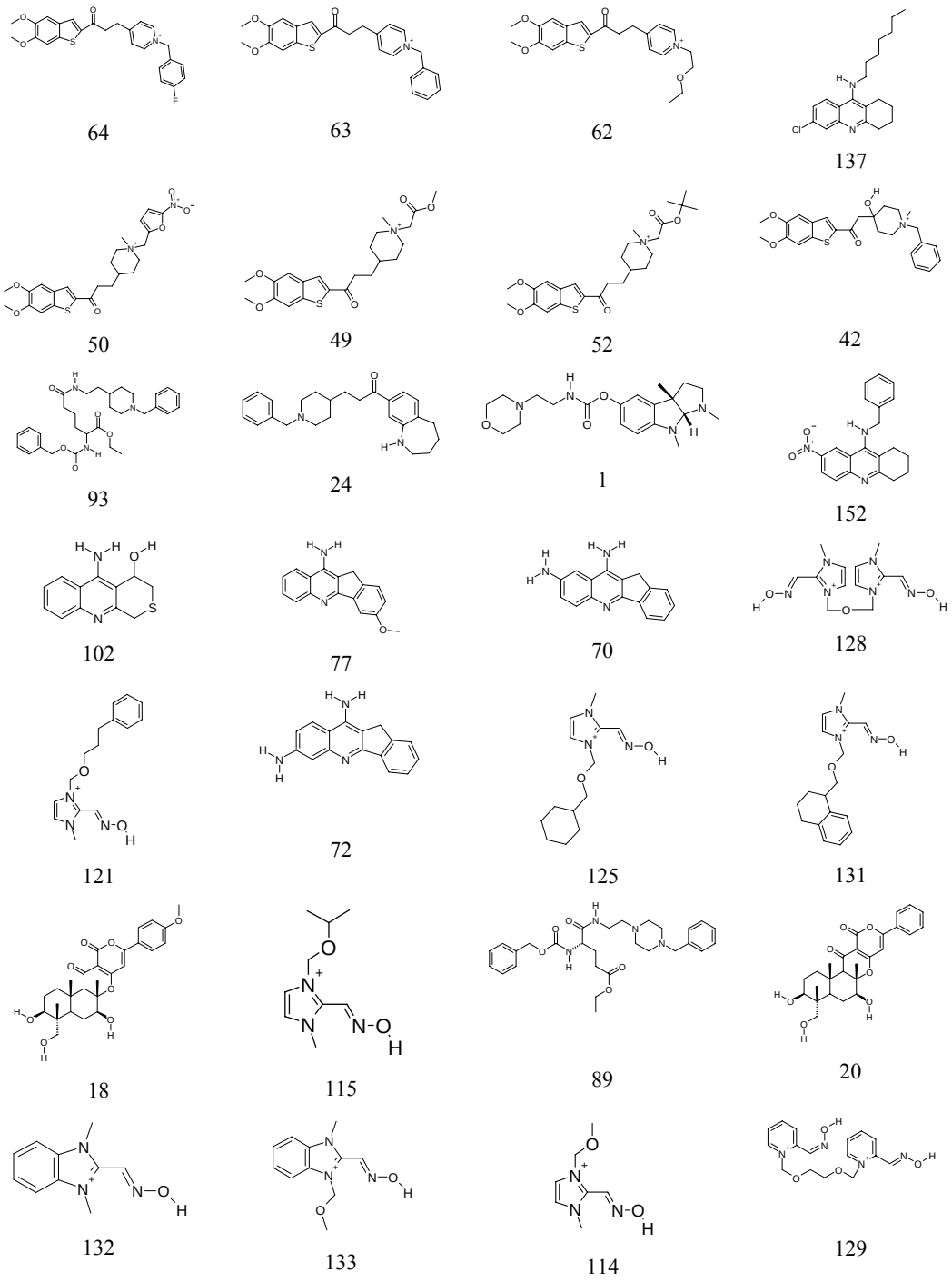

Figure 8.2: Training set molecules considered in *HypoGen* model generation. Numbers correspond to the compounds serial number.

8.2.3 *Docking (GOLD)*

The crystal structure of AChE (PDB ID 1B41), human acetylcholinesterase complexed with fasciculin-II, was obtained from the protein databank [8.27, 8.28]. H–atoms were added to the protein in the hydrogen adding option in MOE. The complexed ligand fasciculin-II was removed from the crystal structure, and then subjected to minimization by keeping the heavy atoms rigid. This was carried out in the MOE minimizer with MMFFx force field. This minimized structure was then exported to GOLD for docking.

The compiled data set of 153 compounds were docked into the crystal structure using GOLD software. The active site of human AChE is characterized by a deep and narrow gorge, which penetrates half way into the enzyme; the catalytic site is present about 4 Å from its base [8.27]. A region of 10 Å radius around this gorge was selected as the active site. The default set of parameters were used during docking. For each of the 10 independent Genetic Algorithm (GA) runs, with a selection pressure 1.1, 100,000 GA operations were performed on a set of 5 islands. The population size of 200 individuals was specified. Default operator weights were used for crossover, mutation, and migration of 95, 95 and 10 respectively. To further speed up the calculation, the GA docking was stopped when the top three solutions were within 1.5 Å RMSD of each other. All other values were set to the default. While docking, a limited flexibility is allowed for the hydrogen atoms in the –OH, $–NH_3^+$ substituents of the side chains of Ser, Thr and Lys residues. The water molecules present in the active site were allowed for movement in due course of docking.

8.2.4 *Database screening*

Database generation: Compounds were collected from the ZINC database (zinc5, released Jan 2005) [8.29]. ZINC is a web-based repository database of commercially available compounds. A sample database of 2484652 compounds was built in the MOE database. This database comprises molecules provided by various vendors like NCI (161395), Ambinter (721594), ChemDiv (199997), Asinex (378794), CamBridge (599893), ChomGenex (40659), KeyOrganics (26932), LifeChemical (64660), Pubchem (57858), Maybridge (49803), Nanosyn (83067). The functional groups of each compound were mapped with the PCHD pharmacophore scheme in MOE database.

Database screening: To combine pharmacophore features and docked conformation, the features generated in the *HypoGen* model were assigned to the best

GOLD solution of compound **64** in the MOE pharmacophore generation module. The PCHD scheme in the pharmacophore builder was used for this purpose. The prepared ZINC database was screened with the 2-D pharmacophore in the MOE database. Generally the 2-D pharmacophore mapping is carried out through the presence or absence of functional groups corresponding to the specified pharmacophore feature. This method avoids 3-D conformation mapping of the molecule. The 3-D coordinates were built for the hit molecules and then subjected to minimization in MOE. The hits retrieved from this 2-D pharmacophore fitting were exported to GOLD for docking and interaction analysis with the receptor (1B41.pdb). For these molecules, calculations were speeded up to 7 times that of default setup. For each of the 5 independent Genetic Algorithm (GA) runs, with a selection pressure 1.1, 1000 GA operations were performed on a set of 3 islands. The population size of 100 individuals was specified. Default operator weights were used for crossover, mutation, and migration of 95, 95 and 10 respectively. The top ranked molecules in the docking were exported to Catalyst for 3-D pharmacophore fitting and screening. A conformation database was prepared for these molecules in Catalyst. The conformations were generated with the fast conformation option of the Catalyst ConFirm module. A maximum of 100 conformations were generated for each molecule within an energy threshold of 20.00 kcal/mol above the global energy minimum. The *HypoGen* model was used for database screening with the "best flexible search" method in Catalyst. The overview of various steps followed in the study is shown in Figure 8.3.

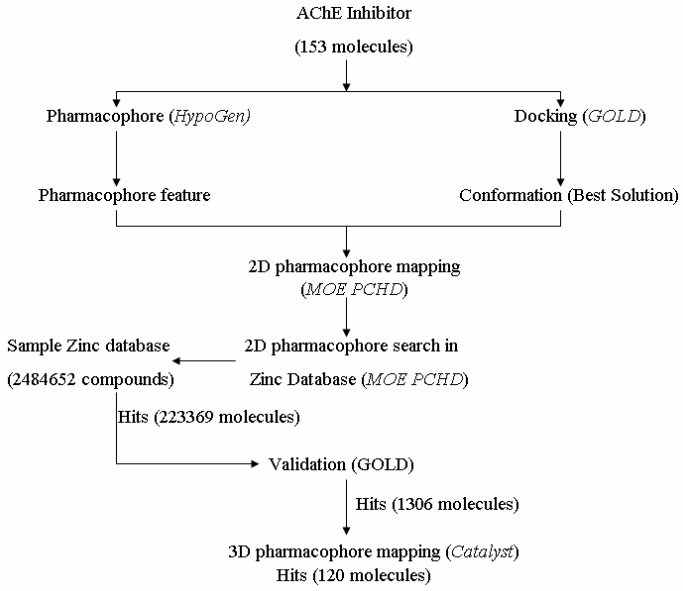

Figure 8.3: Flowchart showing the various steps followed in the study.

All the studies were carried out in *Silicon Graphic Octane 2* and *ORIGIN 200* server. The *Octane 2* work station has a 1GB RAM and the ORIGIN 200 server has a 512 MB RAM. Both work stations are single processor 1020MHz R12000. The sample Zinc database was prepared in a week's time in the *Octane 2* workstation. The assignment of the pharmacophore PCHD scheme and the screening was carried out in 15 days. The docking study for 223369 molecules was performed in 45 days time in the ORIGIN 200 server. The final screening of the top score molecules of GOLD docking was carried out in 3 hours.

8.3 Results and discussion

8.3.1 *HypoGen*

The best pharmacophore model was selected after several iterations of the modeling exercise. A set of ten pharmacophore models with the lowest cost differences were selected for further analysis are and shown in Table 8.1.

Table 8.1: Ranking of pharmacophore models generated by *HypoGen*.

Model	Total cost	Cost difference	RMSD	Training set correlation	Features[a]
1	123.61	53.08	0.97	0.94	HBA, HYA, PI, RA
2	128.76	50.93	1.15	0.93	HBA, HYA, PI, RA
3	130.43	46.26	1.19	0.93	HBA, HYA, HYA, PI, RA
4	130.78	45.90	1.21	0.93	HBA, HYA, PI, RA
5	131.25	45.44	1.22	0.93	HBA, HYA, PI, RA
6	132.27	44.42	1.24	0.92	HBA, HYA, PI, RA
7	133.11	43.58	1.27	0.92	HBA, HYA, HYA, PI, RA
8	133.18	43.51	1.28	0.92	HBA, HYA, PI, RA
9	133.60	43.09	1.27	0.92	HBA, HYA, PI, RA
10	134.19	42.50	1.30	0.91	HBA, HYA, PI, RA

Null cost = 176.69, Fixed cost = 110.24, Configuration = 12.48, All cost units are in bits [a] Hydrogen Bond Acceptor (HBA), Hydrophobic aliphatic (HYA), Positive ionizable (PI), Ring aromatic (RA).

Based on various statistical parameters, model 1 is found to be the best. This model has the lowest RMSD (0.97) and highest correlation coefficient (r = 0.94). The training set compounds are tabulated along with the experimental and predicted activity in Table 8.2. The activities were predicted for the remaining 125 test set compounds using model 1. A correlation coefficient, r = 0.74 was achieved for this set. The correlation between

experimental and predicted inhibitory activities for the training set and the test set compounds is shown in Figure 8.4.

Table 8.2: List of compounds considered in the training set with experimental and predicted pIC_{50} values.

Sl. No.	Compound Sl. No.	Experimental pIC_{50}	Predicted pIC_{50}	Fit value[a]
1	64	8.58	8.05	9.57
2	63	8.33	8.24	9.69
3	62	8.15	7.92	9.24
4	137	7.88	7.29	8.51
5	50	7.49	8.13	8.40
6	49	7.26	8.2	8.49
7	52	7.10	7.95	8.85
8	42	7.04	7.18	8.68
9	93	6.69	6.88	7.71
10	24	6.30	5.52	7.48
11	1	6.15	6.16	7.36
12	152	5.79	4.42	6.55
13	102	5.48	5.01	6.31
14	77	5.36	5.18	6.33
15	70	5.22	4.31	6.30
16	128	5.1	5.03	6.27
17	121	4.82	4.56	6.26
18	72	4.53	4.31	6.31
19	125	4.37	4.88	5.91
20	131	4.25	4.49	6.33
21	18	4.15	4.52	5.75
22	115	4.09	4.5	6.33
23	89	4.06	4.82	6.44
24	20	4	4.52	6.03
25	132	3.91	3.30	4.81
26	133	3.7	3.43	4.91
27	114	3.53	3.63	4.31
28	129	3.46	3.48	4.31

[a] Fit value indicates how well the features in the pharmacophore overlap with the chemical features in the molecule.

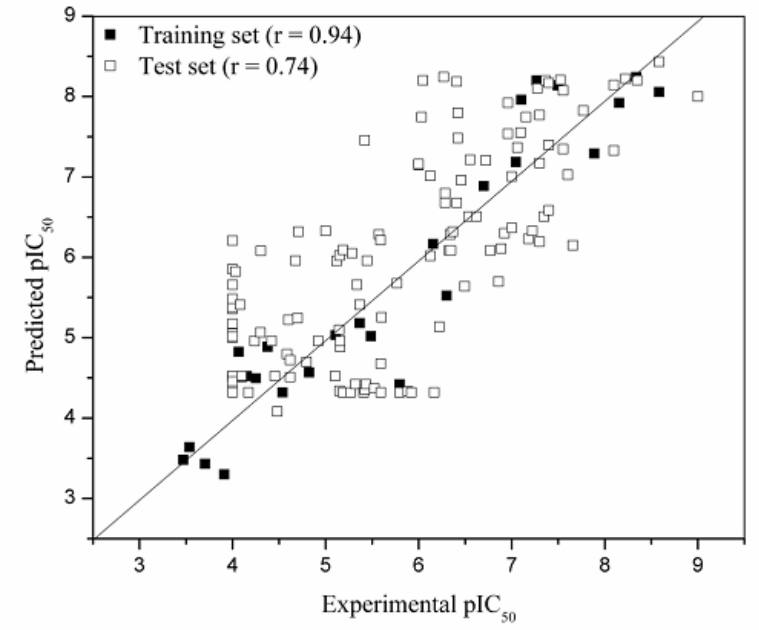

Figure 8.4: Scatter plot of predicted and experimental pIC_{50} value for 28 training set and 125 test set compounds.

The scatter plot suggests that the prediction for 24 molecules is poor. These poorly predicted molecules are mostly inactive. Among these, 16 are false positives and 8 are false negatives. The false positives are velnacrine thiaanalogues (compound **103**, **104**, **105**, **106**, **108**, **111**, **113**), pyripyropene derivative **(16)**, huperazine (**35)**, 11H-indeno-[1,2-b]-quinolin-10-ylamine derivative (**69)** and N-benzylpiperidine aminoacid derivatives (**88**, **90**, **91**, **92**, **95**, **99)**. The reported inhibitory activity for these molecules is IC_{50} > 100 uM (pIC_{50} value 4). Therefore the predicted activities for these molecules are distinct from each other (ranges from 5 to 6.2 pIC_{50} value). Similarly the predicted activities for the 8 compounds [1 compound from the pyridinium derivative (molecule **68),** 6 compounds of 11H-indeno-[1,2-b]-quinolin-10-ylamine derivatives (**71**, **74**, **75**, **76**, **78**, **81**), 1 velnacrine thiaanalogue (**110)**] are the same, i. e. the predicted pIC_{50} value is 4.31. Irrespective of the range of experimental activity (which ranges from pIC_{50} 4 to 6.16), the predicted activity is the same. This is because of the improper mapping of the pharmacophore features in the *HypoGen* model. The two outliers compound **69** and **111** are shown in Figure 8.5. This result shows that the pharmacophore model has limited success in predicting the inhibitory activity of inactive compounds. Since these outliers belong to the inactive set of compounds, it did not hamper the predictive capacity of the pharmacophore model in the higher activity range. In fact one

of the aims of any pharmacophore modeling study is to identify active compound from a pool of inactive compounds.

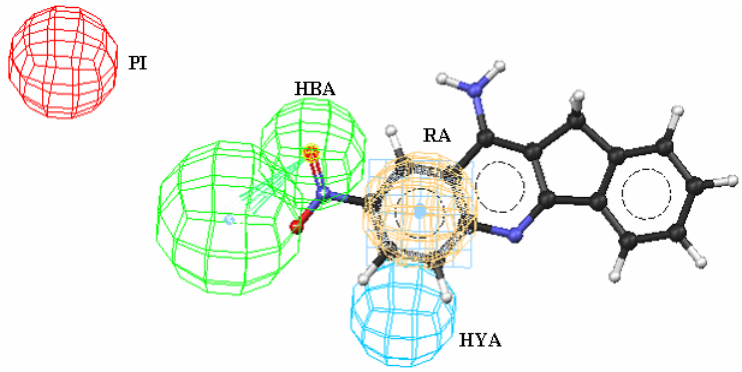

(a)

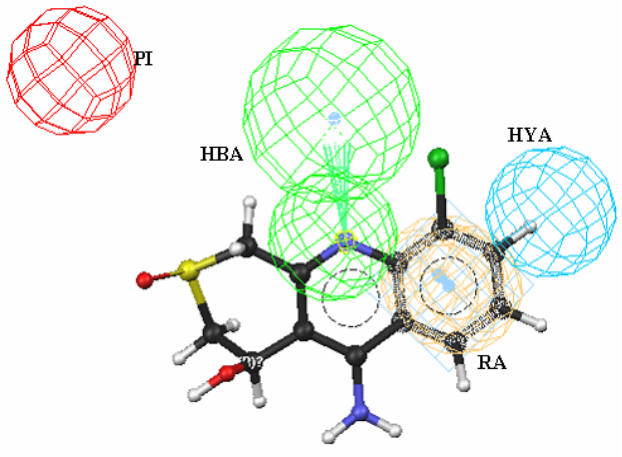

(b)

Figure 8.5: A sample of two outlier (a) **69** and (b) **111** are shown here. Note the improper mapping of pharmacophore features **HYA** and **PI** in both the compounds.

The best pharmacophore model contains five features shown in Figure 8.6. Magenta indicate positive ionizable (PI), green contours are hydrogen bond acceptor (HBA), directionalities shown as conical projections, blue contours indicate hydrophobic aliphatic (HYA), and brown contours represents ring aromatic (RA). The distance matrix for this pharmacophore model is given in Table 8.3.

Table 8.3: Distance matrix (in Å) of the generated *HypoGen* model.

	HBA1 (IP)	HBA1 (PP)	HYA	PI	RA (IP)	RA (PP)
HBA1 (IP)						
HBA1 (PP)	3.0					
HYA	5.4	5.9				
PI	7.6	6.5	12.3			
RA (IP)	3.4	5.4	3.2	11.0		
RA (PP)	4.5	6.2	5.2	11.0	3.0	

IP, initial point on ligand, PP, projected point on the receptor.

The most active molecule **64** in the training set has a fitness score of 9.57 when mapped to the pharmacophore (Figure 8.6*a*), while inactive **129** maps to a value of 4.91 (Figure 8.6*b*). In molecule **64** the HYA feature corresponds to the *meta*-methoxy substitution on the benzothiazole ring. The HBA feature is mapped to the sulfur atom of the benzothiazole ring. RA is mapped onto the aromatic ring of the benzothiazole ring. PI corresponds to the quaternary nitrogen atom of the pyridinium ring. For inactive molecules, HBA is mapped to the methoxy group of the imidazole 3rd position. RA has been mapped to imidazole ring and HYA has been mapped to N-methyl group of imidazole ring. Noteworthy is the absence of the HYA group in molecule **129**. These results suggest a fair performance of the *HypoGen* model to predict the inhibitory activity of AChE inhibitors.

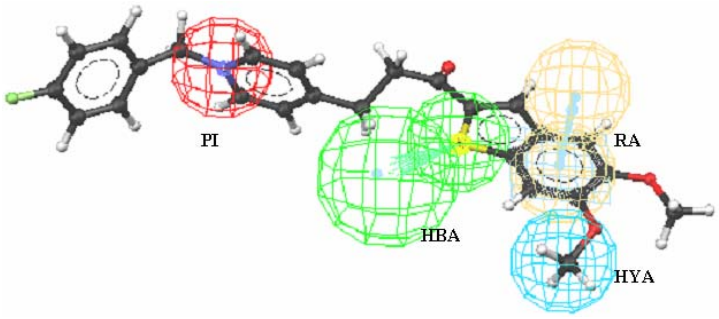

(a)

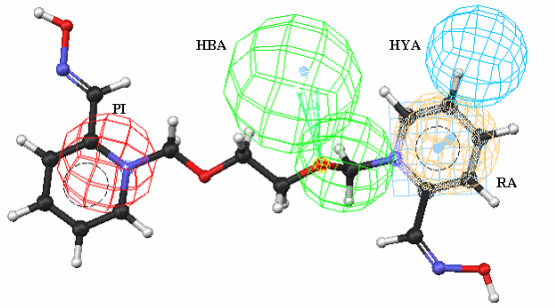

(b)

Figure 8.6: *HypoGen* model map on to: (a) most active molecule **64,** (b) inactive molecule **129**. The green contours represent the positioning of hydrogen bond acceptors (HBA) with their projected points on receptor indicated by conical projections. Blue contours represent the hydrophobic aliphatic (HYA) and brown color corresponds to aromatic (RA), red corresponds to positive ionizable (PI).

8.3.2 *Docking analysis*

The key residues present in the active site gorge are TRP286, LEU76, TYR124, PHE297, THR83, TYR337, PHE338, PHE295, TRP236, TRP86, HIS447, SER203, GLU334 [8.27, 8.30]. All the 153 ligands have been docked into 1B41, using genetic algorithm techniques of Chemscore (GOLD). The docking scores for the best possible conformation and orientation were correlated with observed biological activity (Figure 8.7). Docking results of all AChE inhibitors with 1B41 show better correlation with biological activity; molecules with higher activity exhibited better docking scores. Barring a few inactive molecules, almost all the ligand molecules bind with reasonable scores. These inactive molecules are in the same set of compounds which has experimental activity pIC_{50} > 4, and are shown to be outliers in the pharmacophore model.

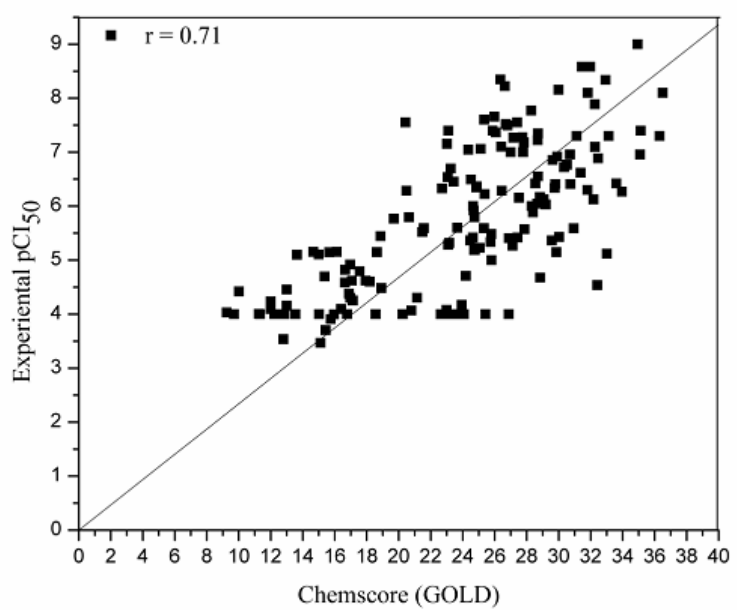

Figure 8.7: Scatter plot of Chemscore (GOLD) vs activity (pIC_{50}) for 153 molecules.

The best docking solutions of molecule **64** and **129** are discussed here to address the ligand–protein interaction of the active/inactive molecule with AChE. Comparative docking scores for molecule **64** and **129** are 31 and 15 respectively, i. e. the docking score of active molecule is twice that of the inactive molecule. The orientation of molecule **64** is such that it completely occupies the active site of AChE as shown in Figure 8.8*a*. At one end, the aromatic ring of the benzothiazole ring interacts with amino acid residue TRP286 through a π-π interaction. This is where the aromatic (RA) nature of pharmacophore is elucidated in the *HypoGen* model. The carbonyl oxygen of ligand interacts with OH^{η} of TYR124 through an O–H···O hydrogen bond (d = 1.7, θ = 145^0). In the case of molecule **129**, the only hydrogen bond found is between the terminal hydroxyl group of the ligand and OH^{γ} of SER125 (d = 1.9, θ = 150^0) Figure 8.8*b*.

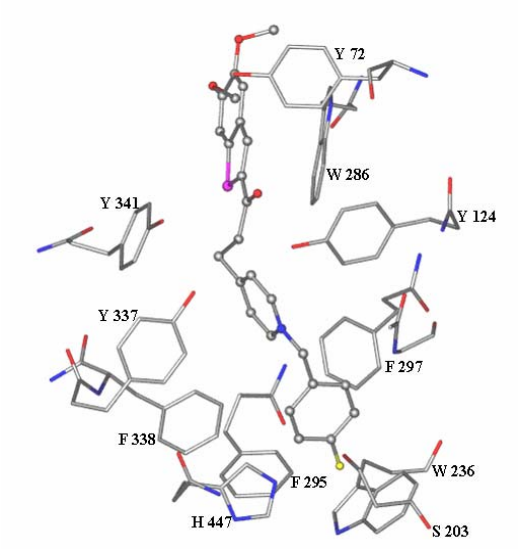

(a)

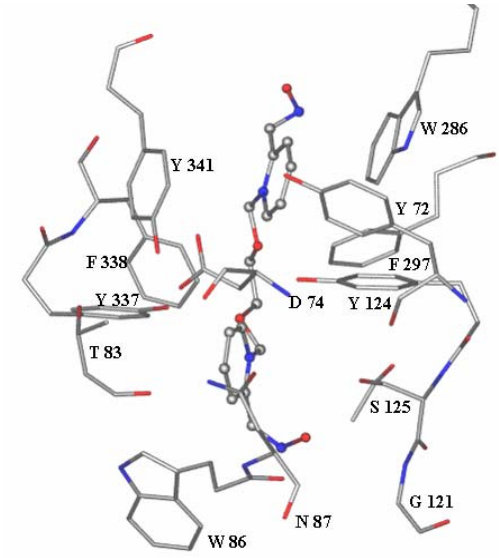

(b)

Figure 8.8: (a) Best GOLD (Chemscore) solutions for molecule **64** and (b) **129** are shown in the active site of 1B41.pdb.

The interactions for best solutions of 153 molecules are also shown in the interaction array through a hit map (Figure 8.9). A detailed analysis of interactions reveals that the interactions observed for these inhibitors can be clustered into 5 categories (Figure 8.10 and Table 8.4).

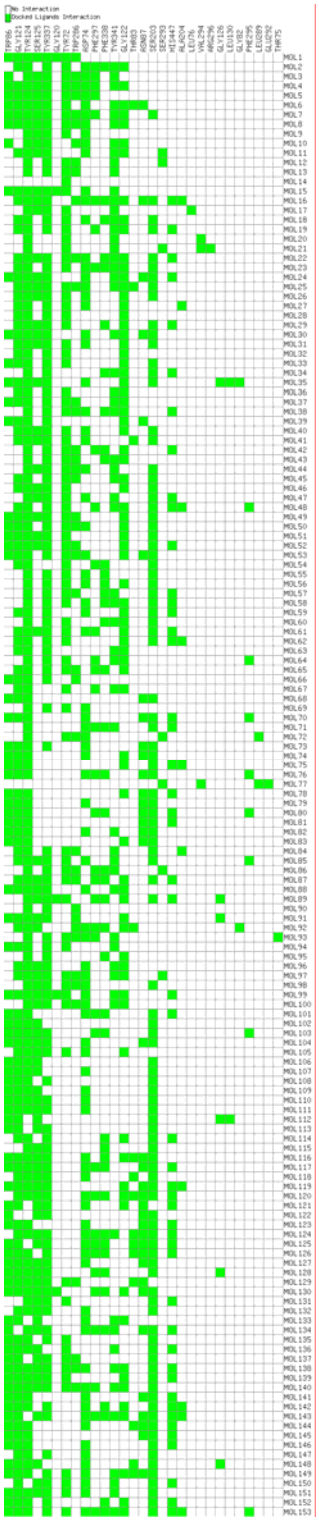

Figure 8.9: Hydrogen bond interaction array shown for the docking solutions of 153 AChE inhibitors. The key residues are shown in the X-axis and molecule serial numbers in the Y-axis.

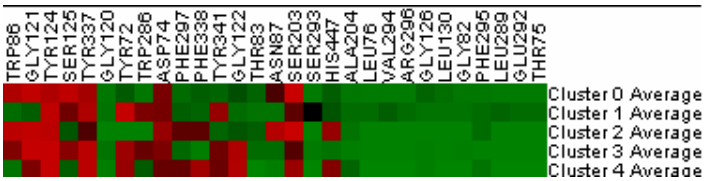
TRP86
GLY121
TYR124
SER125
TYR337
GLY120
TYR72
TRP286
ASP74
PHE297
PHE338
TYR341
GLY122
THR83
ASN87
SER203
SER293
HIS447
ALA204
LEU76
VAL294
ARG296
GLY126
LEU130
GLY82
PHE295
LEU289
GLU292
THR75
Cluster 0 Average
Cluster 1 Average
Cluster 2 Average
Cluster 3 Average
Cluster 4 Average

(a)

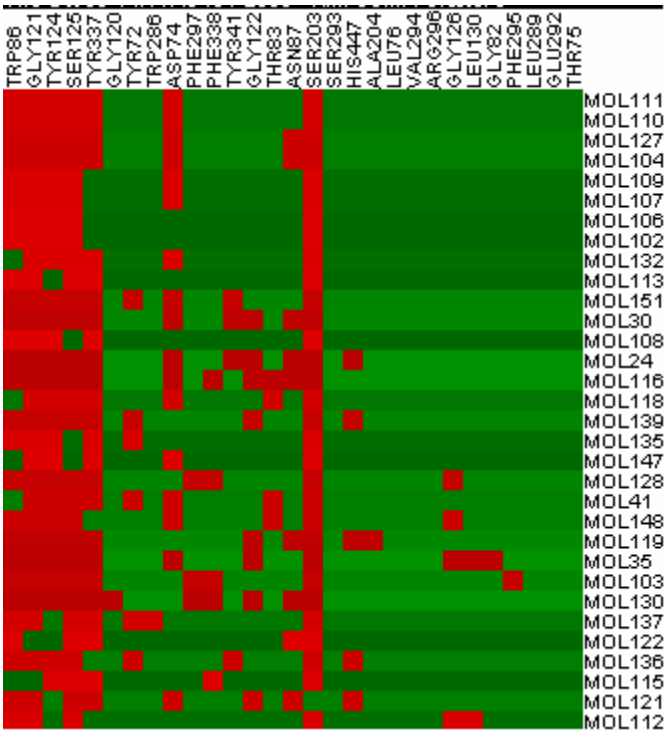
TRP86
GLY121
TYR124
SER125
TYR337
GLY120
TYR72
TRP286
ASP74
PHE297
PHE338
TYR341
GLY122
THR83
ASN87
SER203
SER293
HIS447
ALA204
LEU76
VAL294
ARG296
GLY126
LEU130
GLY82
PHE295
LEU289
GLU292
THR75
MOL111
MOL110
MOL127
MOL104
MOL109
MOL107
MOL106
MOL102
MOL132
MOL113
MOL151
MOL30
MOL108
MOL24
MOL116
MOL118
MOL139
MOL135
MOL147
MOL128
MOL41
MOL148
MOL119
MOL35
MOL103
MOL130
MOL137
MOL122
MOL136
MOL115
MOL121
MOL112

(b)

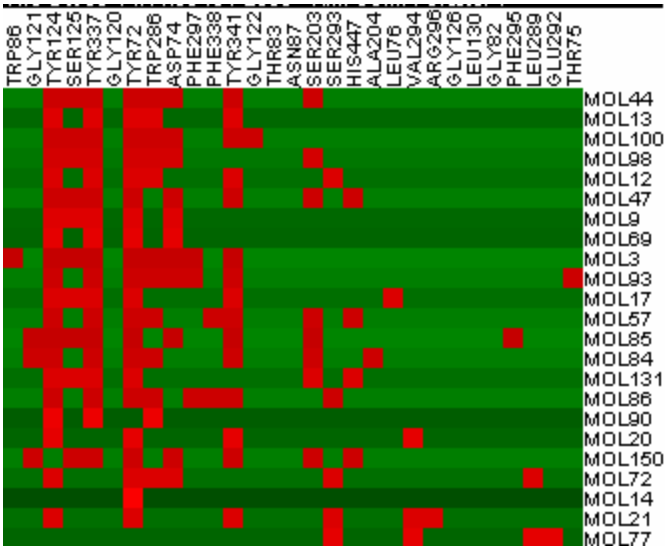
TRP86
GLY121
TYR124
SER125
TYR337
GLY120
TYR72
TRP286
ASP74
PHE297
PHE338
TYR341
GLY122
THR83
ASN87
SER203
SER293
HIS447
ALA204
LEU76
VAL294
ARG296
GLY126
LEU130
GLY82
PHE295
LEU289
GLU292
THR75
MOL44
MOL13
MOL100
MOL98
MOL12
MOL47
MOL9
MOL69
MOL3
MOL93
MOL17
MOL57
MOL85
MOL84
MOL131
MOL86
MOL90
MOL20
MOL150
MOL72
MOL14
MOL21
MOL77

(c)

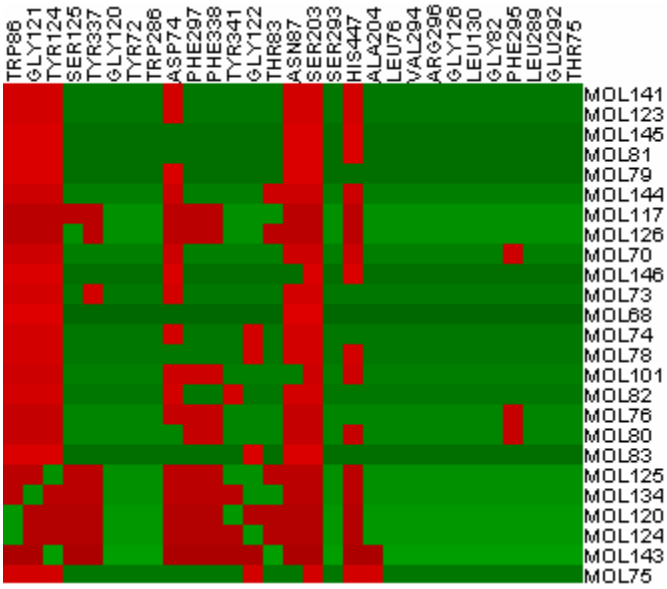
TRP86
GLY121
TYR124
SER125
TYR337
GLY120
TYR72
TRP286
ASP74
PHE297
PHE338
TYR341
GLY122
THR83
ASN87
SER203
SER293
HIS447
ALA204
LEU76
VAL294
ARG296
GLY126
LEU130
GLY82
PHE295
LEU289
GLU292
THR75
MOL141
MOL123
MOL145
MOL81
MOL79
MOL144
MOL117
MOL126
MOL70
MOL146
MOL73
MOL68
MOL74
MOL78
MOL101
MOL82
MOL76
MOL80
MOL83
MOL125
MOL134
MOL120
MOL124
MOL143
MOL75

(d)

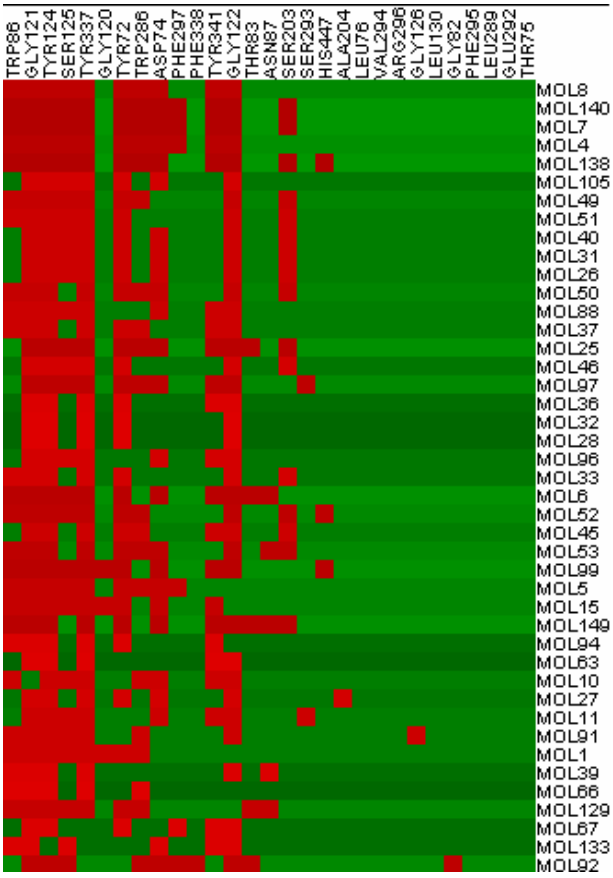
TRP86
GLY121
TYR124
SER125
TYR337
GLY120
TYR72
TRP286
ASP74
PHE297
PHE338
TYR341
GLY122
THR83
ASN87
SER203
SER293
HIS447
ALA204
LEU76
VAL294
ARG296
GLY126
LEU130
GLY82
PHE295
LEU289
GLU292
THR75
MOL8
MOL140
MOL7
MOL4
MOL138
MOL105
MOL49
MOL51
MOL40
MOL31
MOL26
MOL50
MOL88
MOL37
MOL25
MOL46
MOL97
MOL36
MOL32
MOL28
MOL96
MOL33
MOL6
MOL52
MOL45
MOL53
MOL99
MOL5
MOL15
MOL149
MOL94
MOL63
MOL10
MOL27
MOL11
MOL91
MOL1
MOL39
MOL66
MOL129
MOL67
MOL133
MOL92

(e)

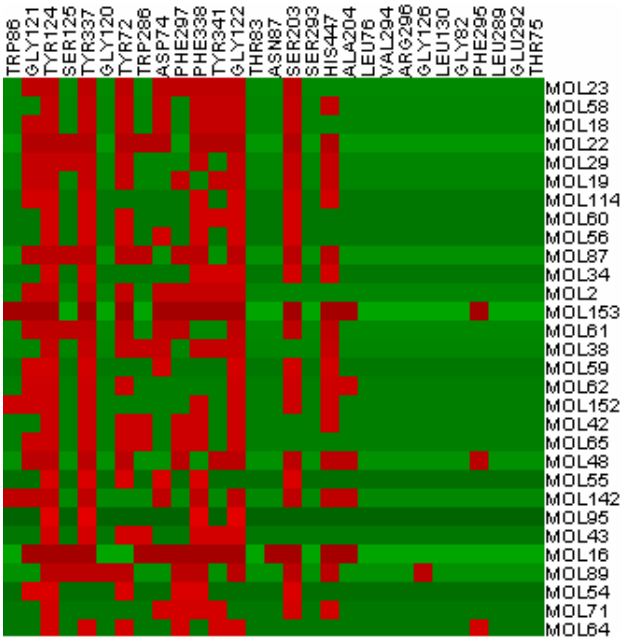

(f)

Figure 8.10: Docked 153 ligands are clustered in to 5 category based on hydrogen bond interaction in the active site of AChE. Average of the interaction observed for each cluster is shown in the hitmap. (a) The X-axis represents key residues of the active site while the cluster code/molecule is shown in Y. The individual member of each clusters are represented by separate hit maps. (b) Cluster 0, (c) Cluster 1, (d) Cluster 2, (e) Cluster 3, (f) Cluster 4.

Table 8.4: Classification of compounds based on the hydrogen bond observed in the active site in docking study. Compound classified in each cluster are represented through majority basis, e. g. Cluster 3 and 4 contains most of the active molecule present in the dataset. Similarly cluster 0 contains mostly Tacrine and Velnacrine derivatives along with other class compounds. Also listed are the interacting residues in the active site of AChE.

Cluster code	Compound class	Key residues
0	Tacrine and Velnacrine derivatives	TRP86, GLY121, TYR124, SER125, TYR337, ASP74, ASN87, SER203
1	Pyripyropene, 11H-indeno-[1,2-b]-quinolin-10-ylamine derivatives, N-benzylpiperidine aminoacid derivatives	TYR124, SER125, TYR337, TYR72, TRP286, ASP74, TYR341, SER203, SER293
2	11H-indeno-[1,2-b]-quinolin-10-ylamine derivatives, 1-(alkoxymethyl)-2-[(hydroxyimino)methyl]-3-methylimida zolium halides, Velnacrine derivatives	TRP86, GLY121, TYR124, TYR337, ASP74, PHE297, PHE338, ASN87, SER203, HIS447
3	Morpholinoalkylcarbamoyloxyeseroline, E2020 Analogues, Piperidinium and Pyridinium Agents, N-benzylpiperidine aminoacid, Tacrine derivatives	TRP86, GLY121, TYR124, SER125, TYR337, TYR72, ASP74, TYR341, GLY122, SER203
4	Pyripyropene, E2020 Analogues, Piperidinium and Pyridinium Agents, Tacrine derivatives	GLY121, TYR124, TYR337, TYR72, ASP74, PHE297, PHE338, TYR341, GLY122, SER203, HIS447

Both active and inactive compounds show hydrogen bond interactions with key amino acid residues like TRP86, GLY121, TYR124, SER125, TYR337, SER203. Among these residues TYR124 and SER125 seems to have conserved interactions with all the compounds.

8.3.3 *Comparative study of pharmacophore and docking*

On the basis of pharmacophore features, *HypoGen* model complements the crucial interactions observed in the GOLD docked solutions. HBA is shown to have hydrogen bond interactions with TYR124 (Figure 8.11). The ring aromatic (RA) of the pharmacophore model has π-π interactions with amino acid residue TRP286. The positive ionizable (PI) or cation is an important pharmacophore feature which interacts with TRP86.

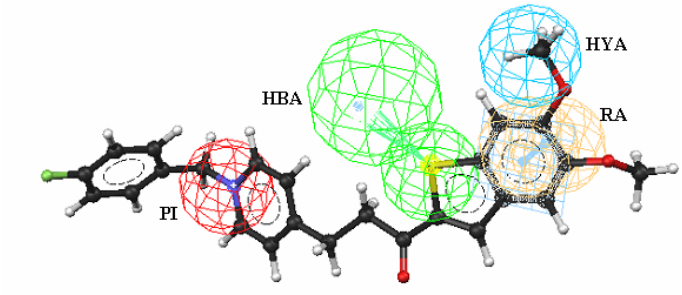

Figure 8.11: *HypoGen* model map on to GOLD best solution for molecule **64**. Pharmacophore annotations are also shown adjacent to pharmacophore features.

The conformation of ligand and protein in 3D space is vital for proper complex formation. It has been recently reported that the bioactive conformations of the ligand depends on molecular weight, number of rotatable bonds etc [8.31, 8.32]. For any computational tool, it is a challenge to generate the bioactive conformation. However limited success has been achieved through various conformation generation tools. In this context the conformation obtained from *HypoGen* model is very similar to conformation obtained in docking solutions, e.g. the RMSD between the GOLD best solution and the *HypoGen* conformation for molecule **64** is 0.91 Å shown in Figure 8.12.

Figure 8.12: RMSD between GOLD best solution (red) and *HypoGen* conformation (green) for molecule **64**.

8.3.4 *Database screening*

Screen 1: The pharmacophore model generated using PCHD pharmacophore scheme was subjected to a 2D pharmacophore search in the sample Zinc database of 2484652 compounds. This search resulted in 223369 hits. These hits are structurally very similar to known inhibitors. Therefore the complementarity between the hits and receptor were studied through docking.

Screen 2: The retrieved hits were subjected to docking using the GOLD software. This study further enhances the quality of hits in terms of complementarities with receptor. The docking score for these compounds ranges from –50 to 50. The score for top ranked hits were well above the 153 AChE inhibitors. A set of 1306 top ranked hits (docking score above 40) were found to be suitable for further interactions analysis.

Screen 3: Molecules with top ranked GOLD scores (1306 molecules) were again mapped and screened with the *HypoGen* model. The number of hits found in this exercise was 120. A comparative analysis of experimental pIC_{50} values for 153 inhibitors and predicted pIC_{50} for 120 hits are shown in Figure 8.13. Similarly the docking scores for this set of compounds are shown in Figure 8.14. The predicted pIC_{50} values for the majority of hits are in the range of 6-7. About five molecules have predicted $pIC_{50} > 7$. This is comparable to all known inhibitors. Also the docking scores for 120 hits are well above the scores observed for the 153 AChE inhibitors. This suggests that the hits encountered in the database mining have better fitness scores compared to experimentally known 153 inhibitors and may be deemed to show inhibitory activity against AChE. As a representative of 120 hits from ZINC database, samples of four hits are shown in Figure 8.15.

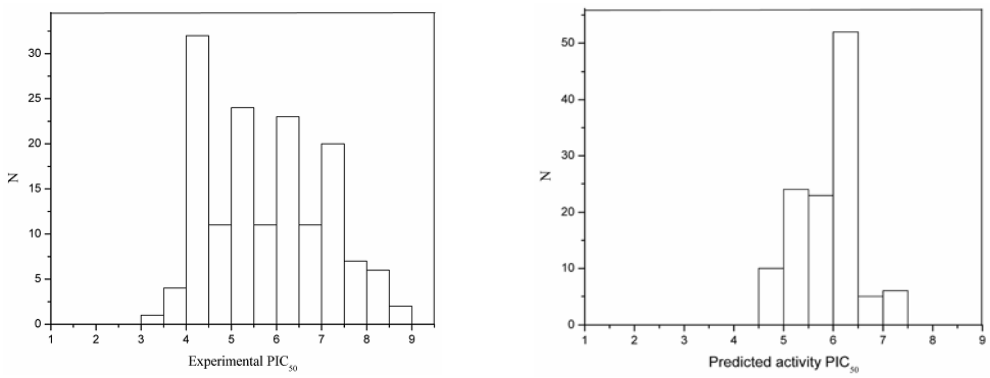

(a) (b)

Figure 8.13: Frequency distribution of pIC_{50} for experimental activity for (a) 153 molecules, and (b) predicted activity for 120 hits.

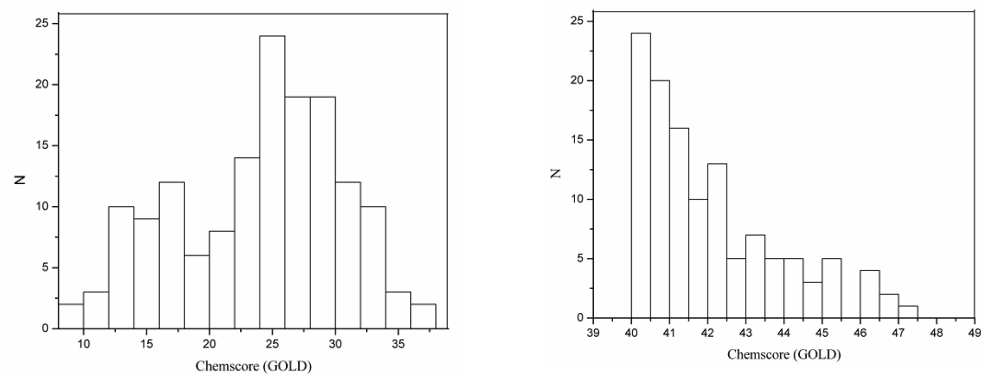

(a) (b)

Figure 8.14: Frequency distribution of Chemscore (GOLD) for (a) known 153 AChE inhibitors, and (b) 120 hits from ZINC database.

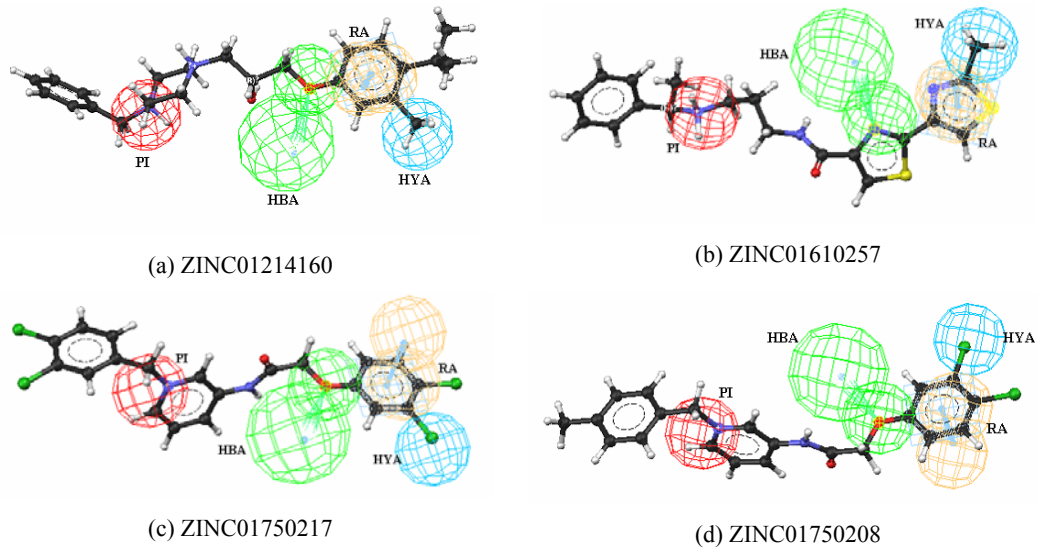

(a) ZINC01214160 (b) ZINC01610257

(c) ZINC01750217 (d) ZINC01750208

Figure 8.15: *HypoGen* model map on to a sample of four top ranked molecules of the 120 hits from ZINC database. The respective ZINC codes are mentioned. The predicted pIC_{50} values are as follows (a) 7.44, (b) 7.15, (c) 7.13 and (d) 7.07.

8.4 Conclusions

The present study describes a rational drug design approach of AChE inhibitors for the treatment of Alzheimer's disease. Various molecular modeling methods such as pharmacophore modeling, molecular docking and virtual screening were successfully implemented to identify possible inhibitors. A diverse set 153 known inhibitors were used to understand pharmacophore features required for AChE inhibitory activity. A reasonably good pharmacophore model was generated using the *HypoGen* module of Catalyst. Regression analysis between pharmacophore features and experimental activity for this set of compounds was carried out successfully. Pharmacophore model containing a hydrophobic aliphatic, ring aromatic, hydrogen bond acceptor and positive ionizable features best describe the inhibitory activity of AChE inhibitors. A molecular docking study of inhibitors with X-ray structure of human AChE revealed key hydrogen bond interactions in the active site. Each compound class seems to have specific hydrogen bond interactions with the active site. These interactions are classified into five clusters based on interacting residues. The most common residues observed in all clusters are TRP86, GLY121, TYR124, SER125, TYR337, TYR72, SER203, TRP286, ASP74, PHE297, PHE338, TYR341, GLY122, ASN87, and HIS447. The important features elucidated in the pharmacophore modeling are complemented through the docking study. Interactions between inhibitor and amino acid residues TRP286, TYR124/125, TRP86 complement ring aromatic, hydrogen bond acceptor and positive ionizable features of the pharmacophore model. The inhibitor conformations generated in the pharmacophore modeling are very similar to conformations obtained in docking. Knowledge obtained in pharmacophore modeling and docking study was used to build a composite model. Initial 2-D pharmacophore screening of composite model followed by molecular docking and 3-D pharmacophore mapping resulted in 120 plausible inhibitors from ZINC database. This short list of compounds have good docking score, reflecting better complementarity with the receptor and predicted activity comparable with the 153 known AChE inhibitors. Thus a method of rational drug design approach for AChE inhibitors was designed and validated combining pharmacophore modeling, docking and virtual screening methods.